TROPOSPHERIC STUDIES USING GOME

Maarten C. Krol, Michiel van Weele, and Renata de Winter Sorkina

Institute for Marine and Atmospheric Research Utrecht (IMAU)

Princetonplein 5, 3584 CC Utrecht, The Netherlands

phone: +30 253 77 60, fax: +30 254 3163

email: krol fys.ruu.nl

http://www.fys.ruu.nl/~wwwimau/

ABSTRACT

Photolysis rates are key parameters in tropospheric chemistry research. This study focuses on how the GOME instrument can attribute to the determination of these photolysis rates. The photolysis rate of ozone is strongly influenced by the stratospheric ozone amount. As an example it is shown that the negative trend in statospheric ozone leads to a positive trend in the ozone photolysis rate in the troposphere. Photolysis rates can be calculated if the actinic flux is known as a function of height. It is investigated if the spectral actinic flux can be obtained from the backscattered UV-spectrum observed by GOME. It is concluded that it is important to estimate the angular reflection distribution function for the different scenes. The scene type that can in part be obtained from level-2 GOME products (Total ozone, clouds, surface pressure) determines for a great deal the actinic flux porfile.

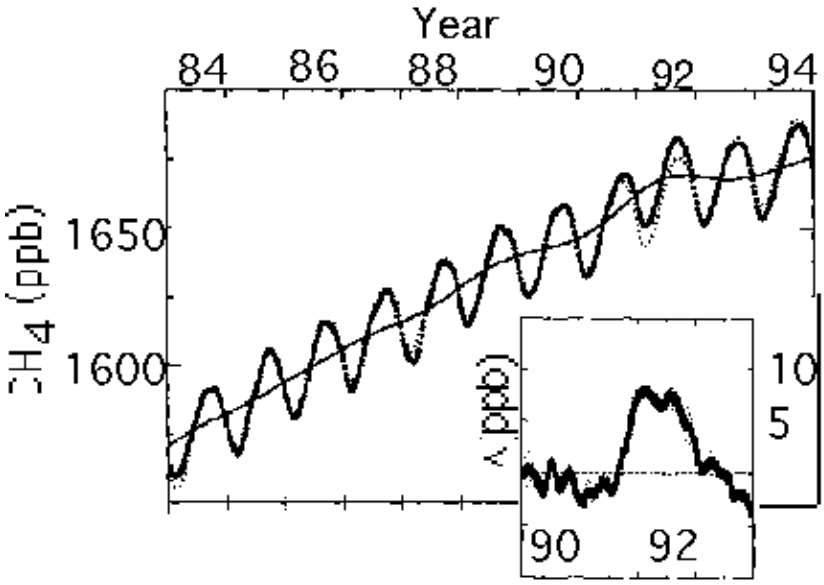

***Figure 1**: Zonally averaged CH_4 mixing ratios for 30-90deg.S The solid line is the deseasonalized trend. The inlay shows the difference between the observations and the long term trend and seasonal cycle (dotted line) (From Dlugokencky et al, 1996).*

1. INTRODUCTION

Tropospheric photolysis rates are of great importance for the chemistry that occurs in this atmospheric layer. Of special importance is the ozone photolysis rate. It should be realised that the photolysis rate is determined by the actinic radiation flux (spherically integrated radiation intensity). If tropospheric ozone is photolysed by UV-B radiation (-320 nm), $O(^1D)$ atoms are formed. Most of these radicals are quenched to ground state O atoms, but a small fraction reacts with water vapour to form two OH radicals. These reactive radicals, which survive for only about one second, oxidise many compounds in the troposphere. OH provides the major sink for CH_4 and CO, as well as for many other compounds.

The determination of the OH concentration on a global scale requires knowledge about the OH precursors, since remote sensing techniques are hampered by the low OH concentration and the interference of H_2O in the spectrally active wavelengths of OH.

Some information about the concentration of OH in the troposphere and its fluctuation can be obtained in an indirect way. For instance, Figure 1 shows the CH_4 concentration as monitored in the Southern Hemisphere (30-90deg.S) as well as the residuals after a parametric fit to the measurements (Dlugokencky et al, 1994, 1996). The positive residuals that are observed during 1991-1992 have been atrributed to lower than normal OH concentrations in the troposphere. The Mt. Pinatubo eruption in June 1991 is held responsible for this observation. During the eruption 20 Mt of SO_2 was injected in the lower stratosphere and upper troposphere. SO_2 absorbes UV radiation and is transformed in sulfate aerosols, which enhance the scattering of radiation. As speculated by Dlugokensky et al (1996), this resulted in lower photolysis rates of ozone in the troposphere, and hence in less OH production.

Since the start of the 1980's stratospheric ozone has declined with several percent, especially at high latitudes. Evidence accumulates that, in response to higher UV fluxes in the troposphere, the tropospheric OH concentration increased. At least part of the rapid decline in CH_4 and CO growth rates during 1992-1993 may be explained by this mechanism, since an additional amount of stratospheric ozone was removed due to heterogeneous processes on the Mt Pinatubo sulfate aerosols (Bekki et al, 1994, Granier et al., 1996).

These two examples show that photolysis is a very important process in the troposphere. It should be modelled properly in order to understand the trends of many trace gases. In the following we will discuss the oppertunities to use remote sensing for the retrieval of photolysis rates in the troposphere.

2. TRENDS IN STRATOSPHERIC OZONE

The stratospheric ozone levels change periodically as part of regular natural cycles such as the 11-year solar cycle, seasons and winds. Over the past two decades human activities have been disrupting the ozone balance. Human production of chlorine-containing chemicals such as chlorofluorocarbons (CFCs) and halons (sources of Bromide) has added a force that destroys stratospheric ozone.

The new version 7 of column ozone data measured by TOMS (Total Ozone Mapping Spectrometer) aboard the Nimbus-7 satellite from November 1978 to April 1993 was used to determine stratospheric ozone depletion trends. The temporal dependency of the ozone column is described by a multiple linear regression model (De Winter-Sorkina, 1995). The model accounts for seasonal variations, the trend in monthly averaged ozone, the quasi-biennual oscillations (QBO), and the 11-year solar cycle.

Figure 2 shows the zonal and monthly mean total ozone trends derived from Nimbus-7/TOMS version 7 data for the entire period. The ozone trends significantly at the 2[sigma] error level are shown with the light shade. The largest ozone loss at mid-latitudes of the Northern Hemisphere occurs in February between 40deg.N and 50deg.N. In the Southern Hemisphere ozone depletion of about 16 % per decade occurs in October between 60deg.S and 70deg.S. In general, the ozone trends derived from the new version 7 TOMS data are about 1-2% per decade less negative than from the old version 6.

3 TRENDS IN PHOTOLYSIS RATES

In order to assess the effect of declining stratospheric ozone levels on the tropospheric photolysis rate of ozone, the rates are calculated both with the 1978/1979 TOMS data and the 1992/1993 data. The influence of the QBO and the solar cycle was removed from the data. An isotropic two-stream radiative transfer model was used in clear sky conditions.

Figure 3 shows the effect of stratospheric ozone depletion on the ozone photolysis rate at the surface in percent per decade. The largest relative trend in the Northern Hemisphere is found in February between 40deg.N and 50deg.N. The effects at high latitudes in the Southern Hemisphere are even larger. The increase in the ozone photolysis rate is in general a factor of about two larger than the decrease in stratopheric ozone. This is due to the slant path of photons trough the ozone column.

The effects are more dramatic at higher altitudes: Trends at 11 km altitude were found to be a factor of 1.6 higher than at the surface.

.

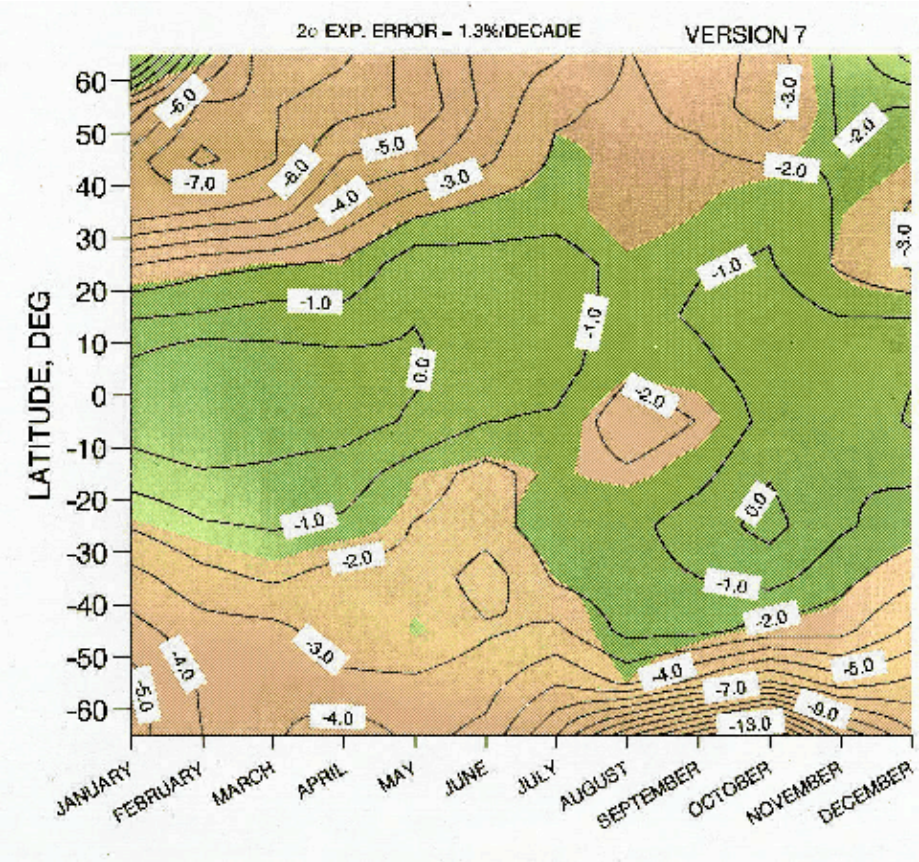

Figure 2*: Seasonal and latitudinal dependency of total ozone trends derived from TOMS version 7 data for the time period 11/1978-04/1993. The trends are given in %/decade. The trends significant at the 2[sigma] level are shown in red (light shade)*

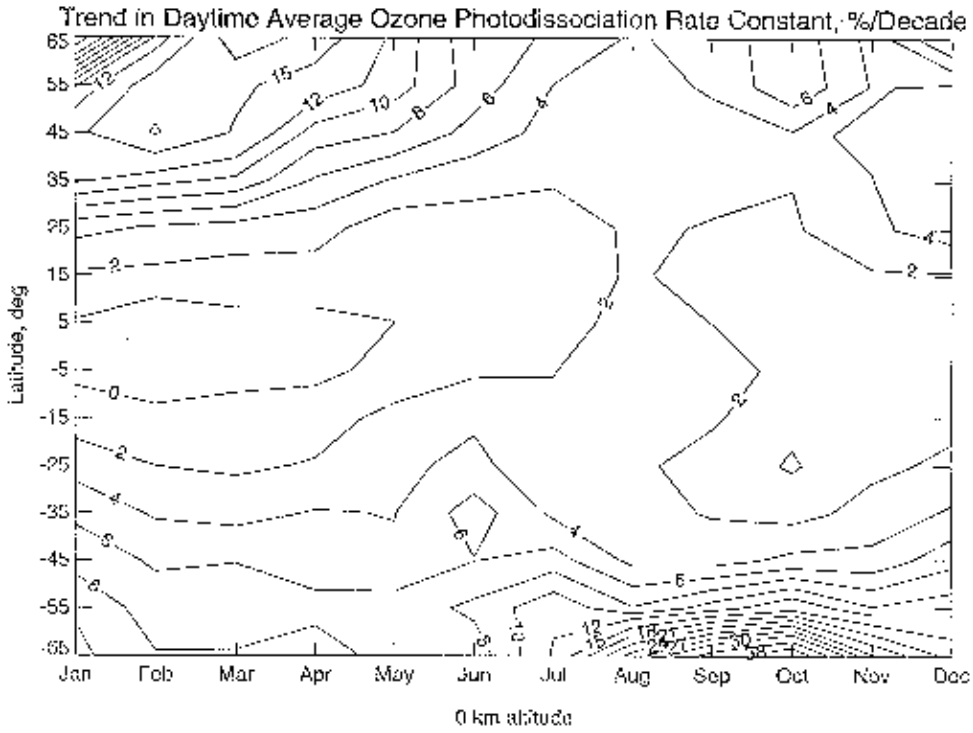

Figure 3*: Seasonal and latitudinal trends in the daytime average ozone photolysis rate constant in %/decade at the surface. Ozone quantum yields proposed by Michelsen (1994) were used.*

4. GOME DATA

The GOME instrument provides an opportunity to retrieve information about tropospheric photodissociation rates. For instance, the retrieved total ozone column can be used to constrain the radiative transfer calculations that are needed for the photolysis rates. Since photolysis rates are also very sensitive for clouds and the surface albedo, other (level-2) products can also be used.

A more appealing way to constrain photolysis rate calculations is to use the level-1 GOME spectra. Therefore we will have a closer look at one track of level-1 data recorded on 28 October 1996 (no. 61028141).

Figure 4 shows this track, from which we will use only the nadir (middle) part. The figure is constructed with the use of the PMD (polarization measurement device) measurements. The ratio PMD3 (600-800nm) /PMD2(400-600nm) is used to obtain information about the scenes. A low ratio generally means low cloud cover over oceans, whereas a high ratio results from either clouds or scenes over the continent. Some level-2 data of this track are presented in Figure 5 as a function of the latitude. The level-2 cloud fraction generally agrees with the PMD measurements. The most important cloud systems at 45N, 20N, and in the Southern Hemisphere over the ocean are clearly visible. The level-2 surface pressure clearly shows the continent and the low surface pressure over the Andes.

Next, we analyse the nadir reflectivity at some specific wavelengths (Figure 6). The reflectivity is identical to the true albedo at the top of the atmosphere if the upward radiation would be isotropically distributed over all zenith angles. The wavelengths are chosen such that they show the effect of different physical processes that influence photolysis rates.

At 310 nm the solar radiation is strongly absorbed by ozone in the stratosphere, but still a significant amount of the radiation enters the troposphere. There, the radiation is scattered by molecules (Rayleigh scattering) and cloud droplets (Mie scattering) before it passes again the ozone layer and finally reaches the GOME instrument. At 320 nm the scattering is almost as important as at 310 nm, but now the amount of absorption by ozone is much smaller. UV-B radiation at about 320 nm contributes most to the ozone photolysis rate in the troposphere. At 360 nm the scattering by air molecules is significantly smaller than at 320 nm, whereas the scattering by large (cloud) particles is practically identical.

At 360 nm there is no ozone absorption. This UV-A radiation is important for the photodissociation of H_2O_2 and NO_2. At 523 nm the scattering by air molecules is small, but scattering by clouds is still about the same as at the shorter wavelengths. Some ozone absorption occurs at 523 nm (Chappuis bands).

Cloud systems can easily be discerned at all wavelengths. For example, the high reflectivity around 15deg.N indicates an optically thick cloud system. Observe that the reflectivity at 523 nm is higher than the reflectivity at 320 nm only in the case of high reflectivity. The explanation is that at high reflectivity both wavelength are reflected strongly, but only 320 nm is affected by ozone absorption.

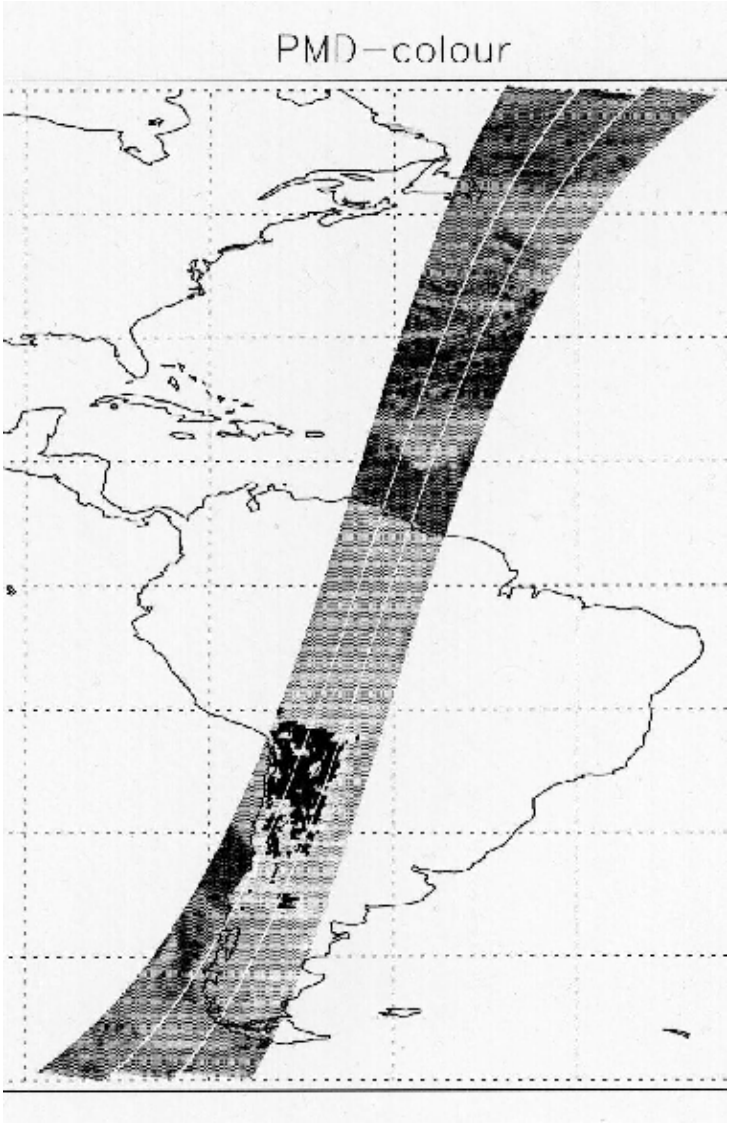

Figure 4*: Gray-scale image of PMD3/PMD2 measured at 28 October 1996 (orbit 61028141). The East Nadir and West pixels are shown, but only the Nadir part will be used. The PMD resolution is 40 km (along track) x 20 km (across track), i.e. 16x the resolution of the GOME spectra. The grid drawn is 15x15 degrees. The black color over the Andes actually means a high PM3/PM2 ratio.*

At 360 nm the Rayleigh scattering adds to the effect of clouds, whereas ozone absorption decreases the reflectivity at 523 nm slightly. Therefore the reflectivity at 360 nm is typically the largest for all scenes. Interestingly, above the ice cap area between 45deg.S and 50deg.S the reflectivity at 523 nm is larger, probably due to the high surface albedo.

Two complete GOME spectra (Figure 7) illustrate the difference between a cloudy scene and a clear sky scene. The selected pixels are close to 15deg.N, one with full cloud cover and the other almost cloud free. Apart from the strong ozone absorption at UV-B wavelengths, the cloudy scene also shows the broadband ozone absorption in the Chappuis bands (520-650nm). The small jumps at about 410 and 600 nm are caused by the serial read-out of the spectrum, i.e. the observed scene is different at the beginning and the end of the read-out (See also GOME validation report, 1996).

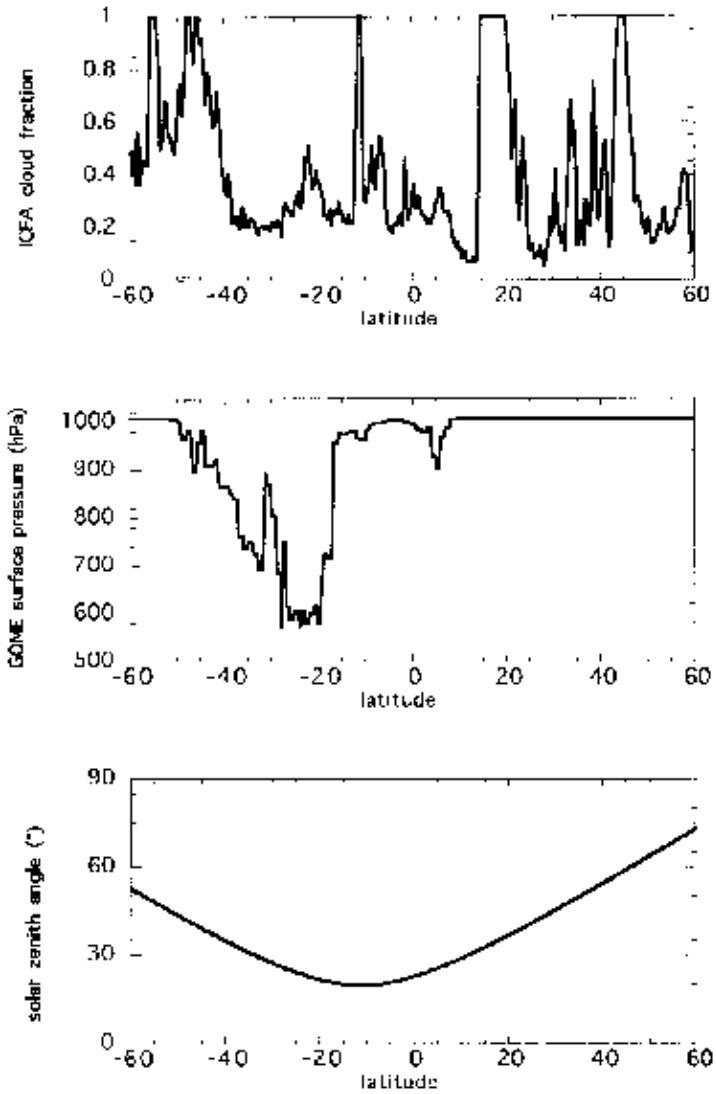

Figure 5*: Level-2 products for the nadir track shown in Figure 4. Top: ICFA cloud fraction; Middle: Surface pressure (climatology); Bottom: Solar zenith angle, calculated along the track.*

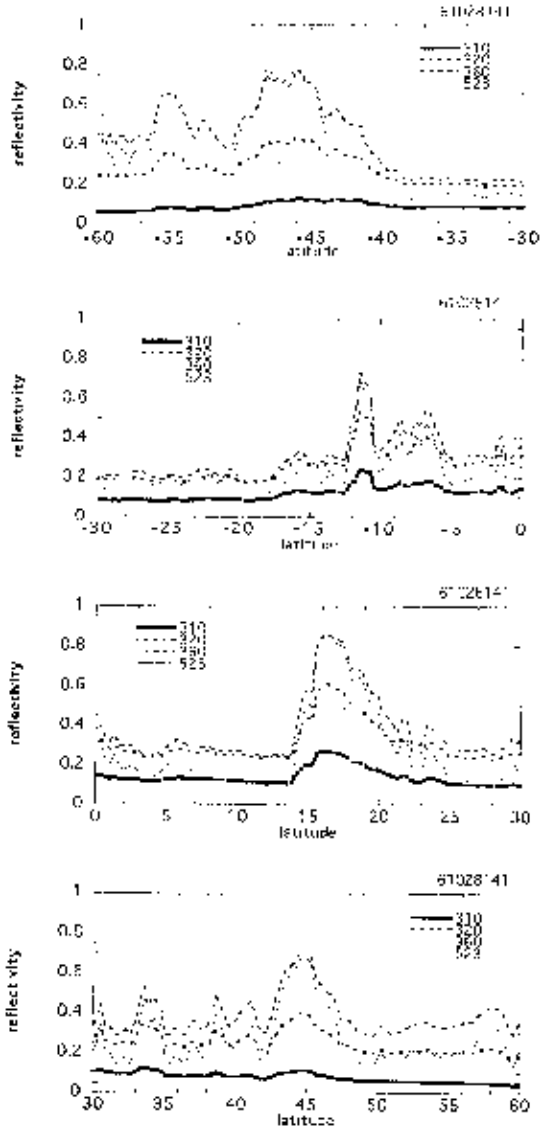

Figure 6*: The reflectivity at the top of the atmosphere at 310, 320, 360, and 523 nm for the nadir track in Figure 4, shown as a function of latitude. The latitude domain is cut into for parts.*

5. RADIATIVE TRANFER CALCULATIONS

In order to get a first indication of the possible photolysis rate retrieval from GOME data, we did some test model calculations. The DISORT model (Stamnes et al., 1988) was used to simulate the radiative transfer at 360 nm. The calculations are by no means meant to be conclusive since the comparison between the output of the radiative transfer model and the nadir radiance measured by GOME was treated very simplistic: The upwelling radiation was assumed to be isotropic.

First we consider a cloud free standard atmosphere and vary the solar zenith angle in the calculations according to the value in each GOME pixel. In the model calculations the surface albedo was taken as zero and the surface pressure as 1000 hPa. Note that ozone absorption is negligible at 360 nm. The results are depicted in Figure 8 and can be compared to the nadir reflectivity measured by GOME at 360 nm.

In the second set of calculations shown in Figure 8 we assume an atmosphere with a homogeneous cloud. The cloud optical thickness is taken as 30 (thick cloud) and the cloud top is positioned at 500 hPa. The calculations may be considered as extreme test situations, since a typical scene is neither cloud free nor homogeneously covered by a thick cloud.

Figure 8 shows that some GOME reflectivities are higher than the model calculations, and some reflectivities are lower. The lower values between 20deg.S and 40deg.S are most likely due to the surface elevation of the Andes that was neglected in the model. The low values north of 40deg.N are most probably due to limitaions of the model calculaions for large solar zenith angles. The upwelling radiation is assumed to be isotropic whereas in reality the limb is normally brighter than the nadir direction for large zenith angles. The opposite is true for cloudy pixels: above a thick cloud the nadir is brighter than the limb, because photons escape most easily perpendicular to the cloud surface. This may be an explanation for the high reflectivity measured around 15deg.N.

These first calculations show that it is important to take the reflection distribution function into account and to identify the scene properly.

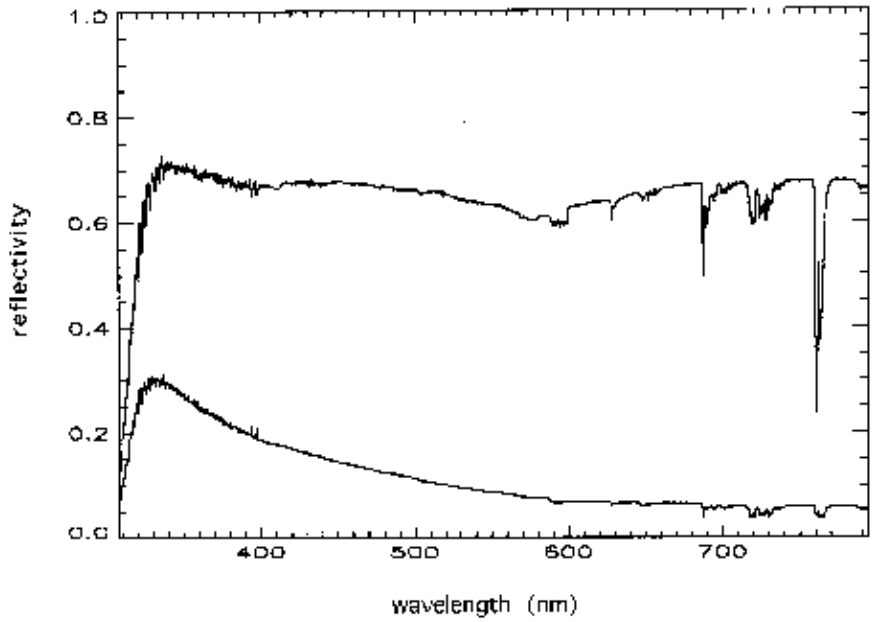

Figure 7*: Two spectra of the Nadir reflectivity for the track in Figure 4. The upper spectrum corresponds to a fully clouded pixel. The lower spetrum is typical for a cloud-free pixel.*

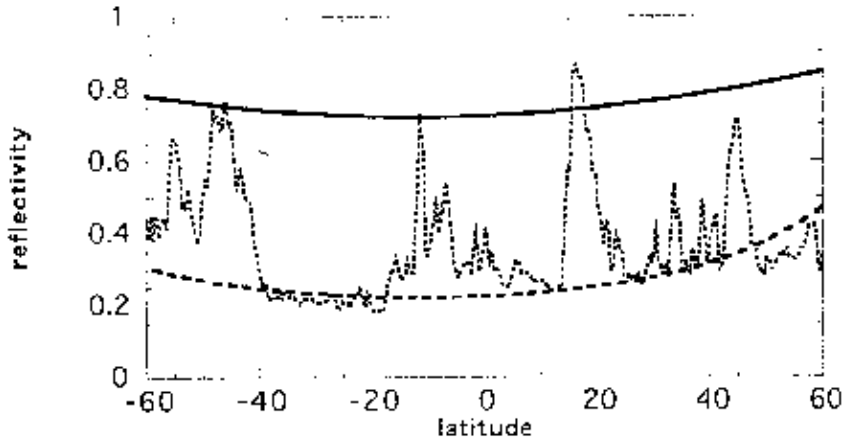

Figure 8*: Short dashes: Nadir reflectivity measured by GOME as a function of latitude; Long dashes: model calculation for cloud free atmosphere; Solid: Model calculation for a cloudy atmosphere (see text).*

6. REFERENCES

Bekki, S., Law, K.S., and Pyle, J.A., 1994: Effect of ozone depletion on atmospheric CH_4 and CO concentrations, Nature, 371, 595-597.

De Winter-Sorkina, R. 1995: Depletion and natural variability of the ozone layer from TOMS observations, RIVM Report no. 722201005, Bilthoven, The Netherlands.

Dlugokencky, E. J., Dutton, E.G., Novelli, P.C., Tans P.P., Masarie, K.A., Lantz, K.O., nd Madronich, S.: 1996: Changes in CH4 and CO growth rates after eruption of Mt. Pinatubo and their link with changes in tropical tropospheric UV flux, Geophys. Res. Lett., 2761-2764.

Dlugokencky, E.J., Steele, L.P., Lang, P.M., and Masarie, K.A.,: 1994: The growth rate and distribution of atmospheric methane, J. Geophys. Res., 99, 17021-17043.

Granier, C., Müller, J.-F., Madronich, S., aand Brasseur, G.P., 1996: Possible causes for the 1990-1993 decrease in the global tropospheric CO abundances: a 3-D sensitivity study, Atmos. Envir., 30, 1673-1682.

Michelsen, H.A., Salawitch, R. J., Wennberg, P.O., and Anderson, J.G., 1994: Production of $O(^1D)$ from photolysis of O_3, Geophys. Res. Lett., 21, 2227-2230.

Stamnes, K.S., Tsay, S.C., Wiscombe W., Jayaweera, K, 1988: Numerical stable algorithm for discrete-ordinate method radiative transfer in multiple scattering and emitting layer media, Appl. Opt., 27. 2501-2509.